IAEA
International Atomic Energy Agency

20th IAEA Fusion Energy Conference
Vilamoura, Portugal, 1-6 November 2004

IAEA-CN-116/TH/8-5Rb

Study of Drift Wave-Zonal Mode System Based on Global Electromagnetic Landau-fluid ITG Simulation in Toroidal Plasmas

N. Miyato [1)], J. Q. Li[2)] and Y. Kishimoto [3)]

1) Japan Atomic Energy Research Institute,
Naka Fusion Research Establishment,
Naka-machi, Naka-gun, Ibaraki, 311-0193, Japan
2) Southwestern Institute of Physics, Chengdu, P. R. China
3) Graduate School of Energy Science, Kyoto University,
Gokasho, Uji, 611-0193, Japan

Study of Drift Wave-Zonal Mode System Based on Global Electromagnetic Landau-fluid ITG Simulation in Toroidal Plasmas

N. Miyato[1)], J. Q. Li[2)] and Y. Kishimoto[3)]

1) Naka Fusion Research Establishment, JAERI, Naka, Ibaraki, 311-0193, Japan
2) Southwestern Institute of Physics, Chengdu, P. R. China
3) Graduate School of Energy Science, Kyoto University, Gokasho, Uji, 611-0193, Japan

e-mail: miyaton@fusion.naka.jaeri.go.jp

Abstract. Using a global Landau fluid code in toroidal geometry, an electromagnetic ion temperature gradient (ITG) driven turbulence-zonal mode system is investigated. Two different types of zonal flows, i.e. stationary zonal flows in a low q (safety factor) region and oscillatory ones in a high q region which are called geodesic acoustic modes (GAM), are found to be simultaneously excited in a torus. The stationary flows efficiently suppress turbulent transport, while the oscillatory ones weakly affect the turbulence due to their time varying nature. Therefore in the low q region where the zonal flows are stationary, the zonal flows are dominant over the turbulence. On the other hand, the turbulence is still active in the high q region where the zonal flows are oscillatory.

1 Introduction

Magnetically confined fusion plasmas contain phenomena with various spatiotemporal scales such as macroscopic MHD modes, ion scale drift waves and small scale electron modes. In most cases each scale has been analyzed separately. However there are phenomena extending into multi-spatiotemporal scales like the formation of an internal transport barrier (ITB) which is necessary for advanced tokamak operation with good confinement properties. The interaction among different turbulence fluctuations is a new issue [1]. It is widely recognized that zonal flows may regulate turbulent structure and then transport. The zonal flows as well as zonal fields can be generated by different scale fluctuations. In core plasma simulations strong steady zonal flows are often observed. At the same time, local fluid simulations and experiments have shown that the zonal flows near the edge have an oscillatory nature due to the coupling with poloidally asymmetric pressure perturbations. The oscillations are called geodesic acoustic modes (GAM) [2, 3, 4]. The oscillatory zonal flows are less effective in suppressing the turbulence than the stationary ones[5]. Hence, the nature of zonal flows in the whole tokamak is important in understanding the ITB physics and controlling the transport. In order to study these issues we have developed an electromagnetic global Landau fluid code in toroidal geometry, which can cover MHD fluctuations and ion scale turbulence. Landau fluid model is useful for turbulence simulations covering a broad range of spatial and temporal scales because the required computational resource is small. Therefore it has been utilized for transport simulation studies including turbulence [6, 7]. In this paper we analyze the change of zonal flow characteristics with the safety factor profile and the nonlinear dynamics between the zonal flows and the turbulence.

2 Model Equations

We use five-field (density n, electrostatic potential ϕ, parallel component of magnetic vector potential A, parallel ion velocity v and ion temperature T) Landau fluid equation system to describe the global electromagnetic turbulence in tokamak plasmas. Compared to the previous resistive drift-Alfvén model (three-field)[8], the five-field model includes a

parallel equation of motion for ion fluid and an ion temperature equation with Hammett-Perkins closure[9]. In the electrostatic limit with adiabatic electrons the five-field model reduces to the three-field ion Landau fluid model. Nonlinear evolution equations for these fields consist of continuity equation

$$\frac{dn}{dt} = a\frac{dn_{eq}}{dr}\nabla_\theta\phi - n_{eq}\nabla_\parallel v + \nabla_\parallel j + \omega_d(n_{eq}\phi - p_e) + D_n\nabla_\perp^2 n, \tag{1}$$

vorticity equation

$$\frac{d}{dt}\nabla_\perp^2\phi = -T_{eq}\frac{a}{n_{eq}}\frac{dn_{eq}}{dr}(1+\eta_i)\nabla_\theta\nabla_\perp^2\phi + \frac{1}{n_{eq}}\nabla_\parallel j - \omega_d\left(T_i + \frac{T_{eq}}{n_{eq}}n + \frac{p_e}{n_{eq}}\right) + D_U\nabla_\perp^4\phi, \tag{2}$$

equation of motion for the ion fluid in the parallel direction

$$\frac{dv}{dt} = -\nabla_\parallel T_i - (1+\tau)\frac{T_{eq}}{n_{eq}}\nabla_\parallel n - \beta T_{eq}\frac{a}{n_{eq}}\frac{dn_{eq}}{dr}(1+\eta_i+\tau)\nabla_\theta A + D_v\nabla_\perp^2 v, \tag{3}$$

equation of motion for the electron fluid in the parallel direction or Ohm's law

$$\beta\frac{\partial A}{\partial t} = -\nabla_\parallel\phi + \tau\frac{T_{eq}}{n_{eq}}\nabla_\parallel n + \beta\tau T_{eq}\frac{a}{n_{eq}}\frac{dn_{eq}}{dr}\nabla_\theta A + \sqrt{\frac{\pi}{2}\tau\frac{m_e}{m_i}}|\nabla_\parallel|\left(v - \frac{j}{n_{eq}}\right) - \eta j, \tag{4}$$

ion temperature equation

$$\begin{aligned}\frac{dT_i}{dt} &= T_{eq}\frac{a}{n_{eq}}\frac{dn_{eq}}{dr}\eta_i\nabla_\theta\phi - (\Gamma-1)T_{eq}\nabla_\parallel v - (\Gamma-1)\sqrt{\frac{8T_{eq}}{\pi}}|\nabla_\parallel|T_i \\ &\quad + T_{eq}\omega_d\left((\Gamma-1)\phi + (2\Gamma-1)T_i + (\Gamma-1)\frac{T_{eq}}{n_{eq}}n\right) + D_T\nabla_\perp^2 T_i,\end{aligned} \tag{5}$$

and parallel current is related with the magnetic potential through the Ampère's law

$$j = -\nabla_\perp^2 A, \tag{6}$$

where, $p_e = \tau T_{eq} n$, n_{eq} (T_{eq}) is an equilibrium density (ion temperature) normalized by the central value n_c (T_c), $\tau = T_{e0}/T_{i0}$ is a ratio of electron and ion equilibrium temperatures, $\beta = (n_c T_c)/(B_0^2/\mu_0)$ is a half of beta value evaluated on the plasma center, $\eta_i = d\ln T_{eq}/d\ln n_{eq}$, B_0 is a toroidal magnetic field on the magnetic axis and $\Gamma = 5/3$ is a ratio of specific heats. It is noted that an electron Landau damping term is added in the Ohm's law[10]. We assume a circular tokamak geometry (r, θ, ζ), where r is a radius of magnetic surface, θ and ζ are poloidal and toroidal angles, respectively. Then operators are defined as

$$\frac{df}{dt} = \partial_t f + [\phi, f], \quad \nabla_\parallel f = \epsilon\partial_\zeta f - \beta[A, f],$$

$$\omega_d \cdot f = 2\epsilon[r\cos\theta, f],$$

$$[f, g] = \frac{1}{r}\left(\frac{\partial f}{\partial r}\frac{\partial g}{\partial\theta} - \frac{\partial f}{\partial\theta}\frac{\partial g}{\partial r}\right)$$

where $\epsilon = a/R$ is an inverse aspect ratio, a and R are minor and major radii, respectively. Here the normalizations are $tv_{ti}/a \to t$, $r/\rho_i \to r$, $\rho_i\nabla_\perp \to \nabla_\perp$, $a\nabla_\parallel \to \nabla_\parallel$,

$$\frac{a}{\rho_i}\left(\frac{n}{n_c}, \frac{e\phi}{T_c}, \frac{v}{v_{ti}}, \frac{A}{\beta B_0\rho_i}, \frac{T_i}{T_c}\right) \to (n, \phi, v, A, T_i)$$

where $v_{ti} = \sqrt{T_c/m_i}$, $\rho_i = v_{ti}/\omega_{ci}$, $\omega_{ci} = eB_0/m_i$. Artificial dissipations (D_n, D_U, D_v, D_T) are included to damp the small scale fluctuations.

3 Global Structure of Zonal Flows in Tokamak Plasmas

Using the developed global Landau-fluid code, we have performed electromagnetic ITG turbulence simulations. Parameters used in the calculations are R/a=4, ρ_i/a=0.0125, T_e=T_i, β=0.1%, $n_{eq} = 0.8+0.2e^{-2(r/a)^2}$, $T_{eq} = 0.35+0.65(1-(r/a)^2)^2$, $q = 1.05+2(r/a)^2$. The density and temperature profiles are fixed in the calculations. In these parameters a dominant linear instability is the ITG mode which is stabilized by the finite β effect. The numerical calculations are done by Fourier mode expansion in the poloidal and toroidal directions and finite difference in the radial direction. The Fourier modes included in the calculations are ones having resonant surfaces between $0.2 < r/a < 0.8$ in the range of $m \leqq 80$ and $n \leqq 50$, and nonresonant $(m, n) = (0, 0), (1, 0)$ components, where m and n are poloidal and toroidal mode numbers, respectively. Only even toroidal modes are kept to reduce computational time. The number of radial grid is 256.

Figure 1 shows the E×B zonal flows as a function of radius and time (a) and radial variation of the zonal flow frequency spectra (b). Two types of E×B zonal flows are excited, i.e. one is the almost stationary zonal flow in the inner low q region ($r/a \lesssim 0.45$) and the other is the oscillatory one which is called the GAM in the outer high q region ($r/a \gtrsim 0.45$). The frequency change of the zonal flows is clearly seen in FIG. 1(b), in which the pure GAM frequency $f_{\rm GAM} = \omega_{\rm GAM}/2\pi$ and the pure parallel sound frequency of the (m,n)=(1,0) mode $f_{\rm sound} = \omega_{\rm sound}/2\pi$ are also plotted. Here $\omega_{\rm GAM} = \sqrt{2(\Gamma+\tau)T_{eq}}\frac{a}{R}$ which is derived from the zonal flow and the (1,0) pressure perturbation equations without nonlinear terms in $q \gg 1$ and electrostatic limit and $\omega_{\rm sound} = \sqrt{(\Gamma+\tau)T_{eq}}\frac{a}{qR}$ which is from the (1,0) pressure and the (1,0) parallel ion velocity equations in $q \ll 1$ limit[11]. Although the oscillatory zonal flows have small peaks along $f_{\rm GAM}$, large peaks are located between $f_{\rm GAM}$ and $f_{\rm sound}$ lines. Since the GAM is the oscillation between the zonal flow and the (1,0) pressure perturbation, the zonal flows cannot oscillate without the (1,0) pressure perturbations. When $f_{\rm sound}$ is higher than the frequency of the oscillatory zonal flows by decreasing q, the (1,0) pressure perturbations relax along the magnetic field before they change the zonal flow direction. Therefore only the stationary zonal flows can exist in the low q region.

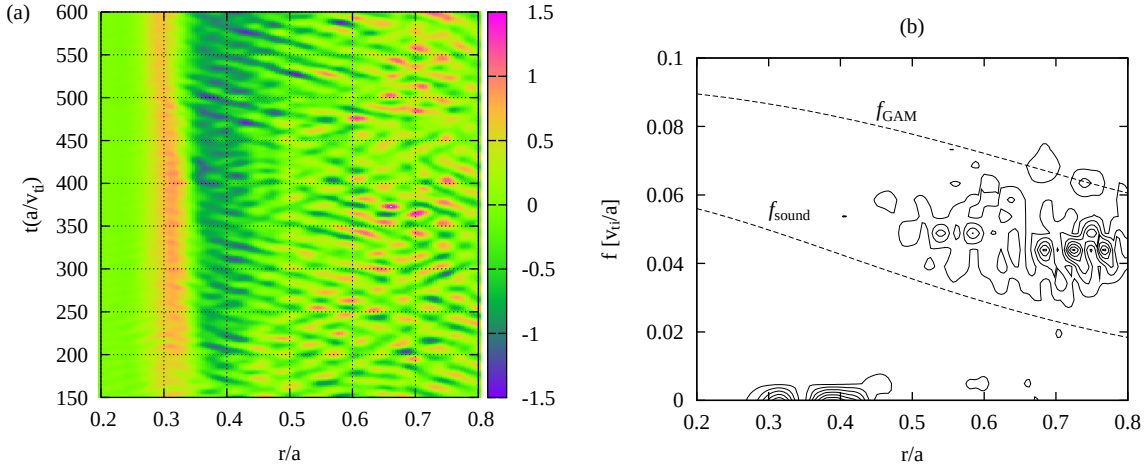

FIG. 1: E×B zonal flows as a function of radius and time (a) and radial variation of zonal flow frequency spectra (b). In the right panel the pure GAM frequency $f_{\rm GAM} = \omega_{\rm GAM}/2\pi$ and the pure parallel sound wave frequency of the (1,0) mode $f_{\rm sound} = \omega_{\rm sound}/2\pi$ are also plotted.

4 Energy Flow between ITG Turbulence and Zonal Flows

It is important to identify the energy transfer channel for the zonal flows. Zonal flow energy is dominated by Reynolds stress, Maxwell stress, and geodesic transfer as described in the following zonal flow energy equation,

$$\frac{\partial}{\partial t}\frac{1}{2}\langle v_E\rangle^2 = \underbrace{-\langle \tilde{v}_{Er}\tilde{\Omega}\rangle\langle v_E\rangle}_{\text{Reynolds}} + \underbrace{\frac{\hat{\beta}}{n_{eq}}\langle \tilde{B}_r\tilde{j}\rangle\langle v_E\rangle}_{\text{Maxwell}} \underbrace{-\frac{2}{n_{eq}}\frac{a}{R}\langle p\sin\theta\rangle\langle v_E\rangle}_{\text{geodesic transfer}}, \tag{7}$$

where $\langle\cdot\rangle$ denotes the flux surface average, $\langle v_E\rangle = \frac{\partial\phi_0}{\partial r}$ is the zonal flow, $\tilde{v}_{Er} = -\frac{1}{r}\frac{\partial\tilde{\phi}}{\partial\theta}$ is the radial E×B drift velocity, $\tilde{\Omega} = \nabla_\perp^2\tilde{\phi}$ is vorticity, $\langle p\sin\theta\rangle$ is the (1,0) pressure perturbation and $p = p_i + p_e = n_{eq}T_i + T_{eq}n + \tau T_{eq}n$ is total pressure. Here a viscous term is neglected. The geodesic transfer is due to the coupling with (1,0) pressure perturbations. Figure 2 shows time averaged zonal flow energy drives as a function of radius. The Reynolds stress drive is positive in almost whole region. The zonal flow energy is supplied from the turbulence by the Reynolds stress as usual. Meanwhile, the geodesic transfer is negative, so that the zonal flow energy goes to the (1,0) pressure perturbations through the geodesic transfer. It is noted that the Reynolds drive in the stationary zonal flow region ($r/a \lesssim 0.45$) is higher than the oscillatory zonal flow region. The Maxwell stress drive is small compared to the other drives, but it increases with β. Therefore the Maxwell stress may affect the zonal flow generation in high β plasmas in which the kinetic ballooning mode is dominant.

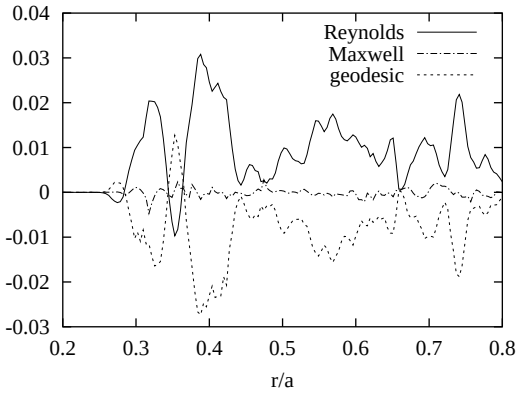

FIG. 2: Time averaged E×B zonal flow energy drives as a function of radius.

The equation describing time evolution of the (1,0) pressure perturbation energy is

$$\frac{\partial}{\partial t}\frac{1}{2}\langle p\sin\theta\rangle^2 = \underbrace{-\langle[\tilde{\phi},\tilde{p}]\sin\theta\rangle\langle p\sin\theta\rangle}_{\text{nonlinear transfer}} + \underbrace{(\Gamma+\tau)p_{eq}\frac{a}{qR}\langle v\cos\theta\rangle\langle p\sin\theta\rangle}_{\text{sound wave}}$$
$$\underbrace{-(\Gamma-1)n_{eq}\sqrt{\frac{8T_{eq}}{\pi}}\frac{a}{qR}\langle T_i\sin\theta\rangle\langle p\sin\theta\rangle}_{\text{Landau damping}} + \underbrace{(\Gamma+\tau)p_{eq}\frac{a}{R}\langle v_E\rangle\langle p\sin\theta\rangle}_{\text{zonal flow}}. \tag{8}$$

Here magnetic nonlinearity ($[\tilde{A},\tilde{v}]$,$[\tilde{A},\tilde{j}]$) related terms, coupling with Alfvén waves ($\langle j\cos\theta\rangle$ term), source terms from the equilibrium pressure gradient and a viscous term are neglected. Figure 3 shows time averaged drives for the (1,0) pressure perturbations $\langle p\sin\theta\rangle$ in the above equation as a function of radius. In the stationary zonal flow region ($r/a \lesssim 0.45$) most of the energy transferred from the zonal flows goes to the (1,0) parallel ion velocity $\langle v\cos\theta\rangle$. On the other hand, the energy channel is different in the oscillatory zonal flow or GAM region ($r/a \gtrsim 0.45$). The energy flow to $\langle v\cos\theta\rangle$ is much smaller than that in the stationary zonal flow region. Instead energy transfer to the ITG turbulence by nonlinear coupling of the electrostatic potential and pressure perturbations is dominant. This is the same result as the drift-Alfvén turbulence simulation in Ref. [4].

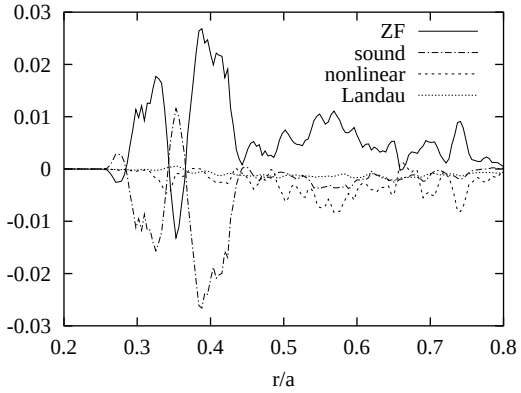

FIG. 3: Time averaged $\langle p \sin\theta \rangle$ energy drives as a function of radius.

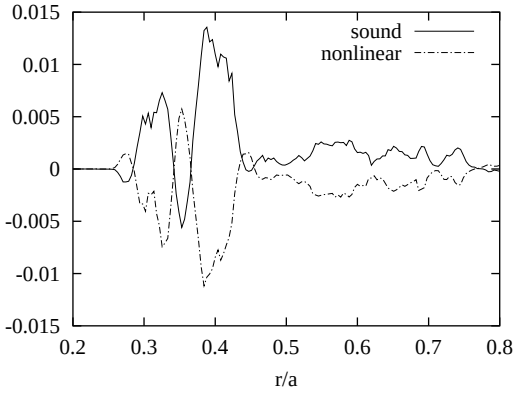

FIG. 4: Time averaged $\langle v \cos\theta \rangle$ energy drives as a function of radius.

Figure 4 shows time averaged $\langle v \cos\theta \rangle$ energy drives in the following equation,

$$\frac{\partial}{\partial t}\frac{1}{2}\langle v\cos\theta\rangle^2 = \underbrace{-\langle[\tilde{\phi},\tilde{v}]\cos\theta\rangle\langle v\cos\theta\rangle}_{\text{nonlinear transfer}} \underbrace{-\frac{1}{n_{eq}}\frac{a}{qR}\langle v\cos\theta\rangle\langle p\sin\theta\rangle}_{\text{sound wave}}, \tag{9}$$

where a magnetic nonlinearity ($[\tilde{A},\tilde{p}]$) related term, a source term from the equilibrium pressure gradient and a viscous term are neglected. The energy transferred from $\langle p \sin\theta \rangle$ tends to balance the nonlinear energy flow to the turbulence, which leads to saturation of the stationary zonal flows[12].

5 Turbulent Transport

Figure 5 shows electrostatic component of ion heat flux $\langle \tilde{T}_i \tilde{v}_{Er} \rangle = -\langle \tilde{T}_i \frac{1}{r}\frac{\partial \tilde{\phi}}{\partial \theta} \rangle$ as a function of radius and time (a) and temporal evolution of the heat flux and the zonal flow energy at $r/a = 0.4$ (b) and $r/a = 0.6$ (c). It is noted that electromagnetic component of ion heat flux is negligibly small. The heat flux in the inner region is effectively suppressed by the stationary zonal flows. As shown in FIG. 5(b), the stationary zonal flows correlate well with the heat flux. When the heat flux increases, subsequently the zonal flow energy increases and the heat flux is reduced by the zonal flow. On the other hand, the heat flux in the outer region with the oscillatory zonal flows is large, and the correlation between the heat flux and the zonal flow is not so strong compared to the stationary zonal flow region (FIG. 5(c)). The effective shearing rate of the oscillatory zonal flows is smaller than that of the stationary zonal flows[5]. Since the frequencies of the oscillatory zonal flows are of the same order as those of the ITG modes, suppression of the ion heat flux by the oscillatory zonal flows is weaker than that by the stationary zonal flows. The oscillatory zonal flows, however, still have suppression effect on the turbulent transport[13]. When the zonal flows are artificially turned off, the heat flux in the oscillatory zonal flow region increases about twice compared with that in the case including the zonal flows.

As a result of the differences between the stationary zonal flows and the oscillatory ones, the tokamak plasma divides into zonal flow dominant region and turbulent region. Figure 6 shows a ratio of the zonal flow energy to the total E×B kinetic energy $(d\phi_0/dr)^2/|\nabla\tilde{\phi}|^2$ as a function of radius and time. In the low q region ($r/a < 0.45$) where the zonal flows are stationary, the ratio is near unity and the zonal flows are dominant over the turbulence.

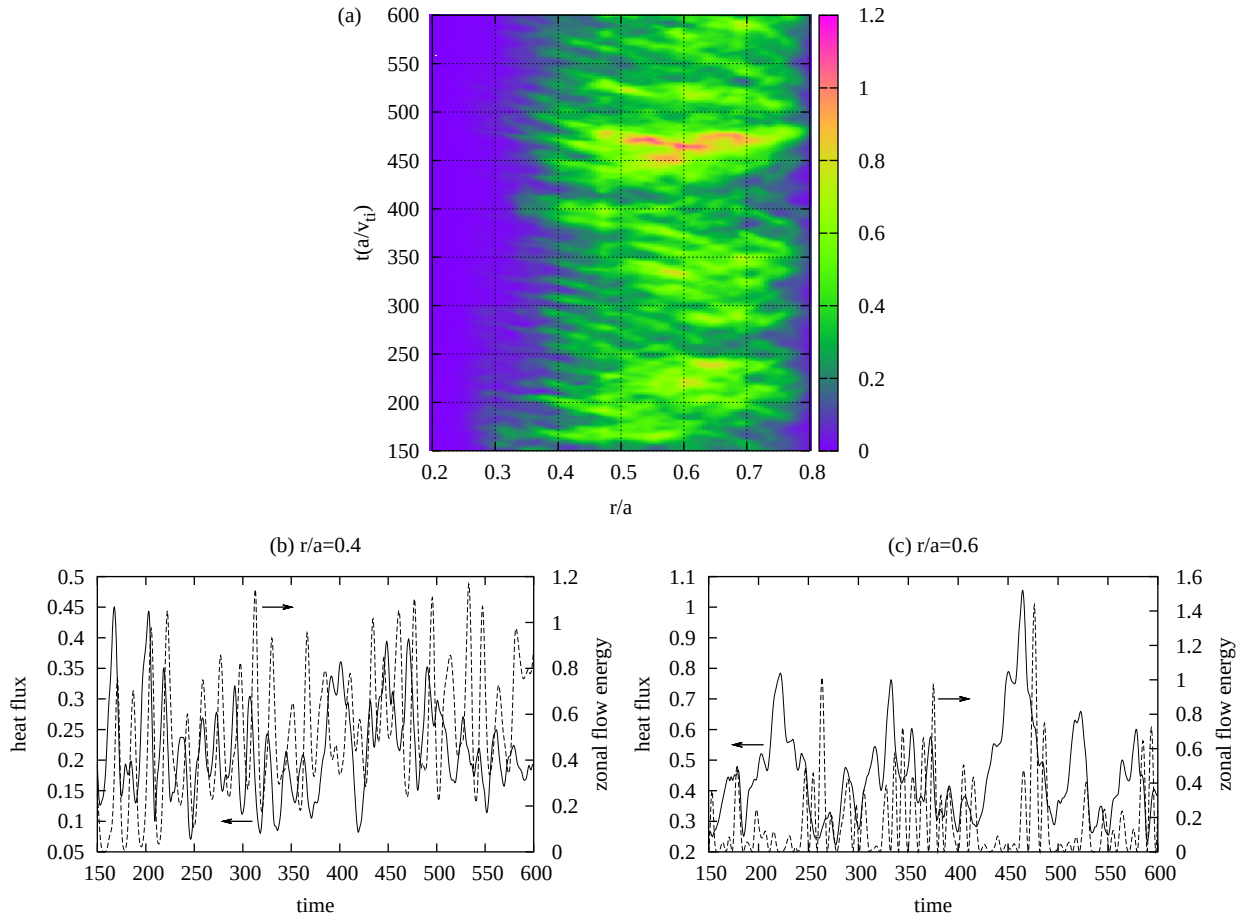

FIG. 5: Electrostatic component of heat flux as a function of radius and time (a), and temporal evolution of heat flux (solid line) and zonal flow energy (dashed line) at r/a=0.4 (b) and r/a=0.6 (c).

On the other hand, the ratio in the high q region ($r/a > 0.45$) where the zonal flows are oscillatory is not so high compared to the stationary zonal flow region.

6 Control of Zonal Flow Behaviour by Safety Factor Profile

The stationary zonal flows in the low q ($q \sim 1$) region are favourable for the suppression of the turbulence. Therefore the turbulent transport will be reduced in wider region of the plasma if the q profile has wider low q region where the stationary zonal flows are excited. We have performed the calculation with the q profile having wider low q region, $q = 1.05 + 2(r/a)^{3.5}$, as shown in FIG. 7. Radial variation of the zonal flow frequency spectra in this case is shown in FIG. 8. The stationary zonal flow region ($r/a \lesssim 0.6$) becomes wider than that in the previous case ($r/a \lesssim 0.45$) because the $f_{\rm sound}$ line shifts to the higher frequency. It is noted that the width of the stationary zonal flows becomes wider due to lower magnetic shear. The electrostatic component of heat flux and the ratio of zonal flow energy to total E×B kinetic energy $(d\phi_0/dr)^2/|\nabla\tilde{\phi}|^2$ in the case with $q = 1.05 + 2(r/a)^{3.5}$ are shown in FIG. 9. It is seen that the heat flux in the stationary zonal flow region is reduced and the zonal flow dominant region extends to $r/a \simeq 0.6$.

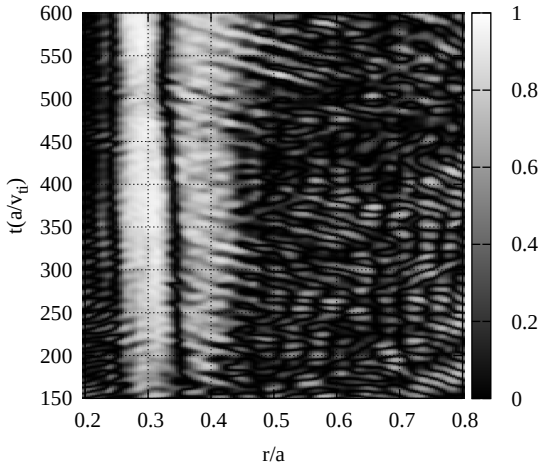

FIG. 6: Ratio of zonal flow energy to total E×B kinetic energy $(d\phi_0/dr)^2/|\nabla\tilde{\phi}|^2$ *as a function of radius and time.*

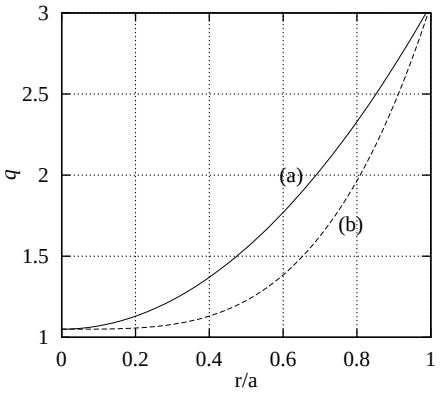

FIG. 7: The q profiles used in the calculations: (a) $q = 1.05 + 2(r/a)^2$ *and (b)* $q = 1.05 + 2(r/a)^{3.5}$.

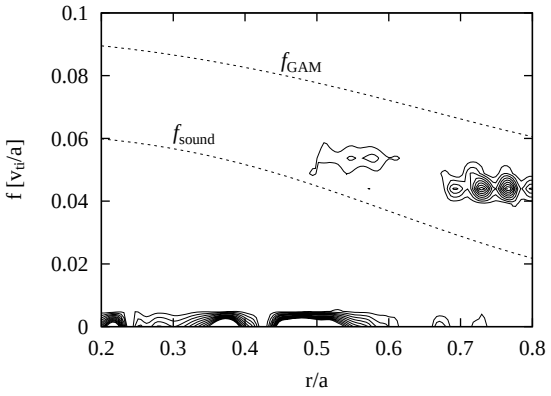

FIG. 8: Radial variation of zonal flow frequency spectra in the case with $q = 1.05 + 2(r/a)^{3.5}$.

7 Summary and Conclusions

We have performed the electromagnetic ITG turbulence simulations in tokamak plasmas using the developed global Landau-fluid code. Two types of zonal flows, stationary and oscillatory modes, are possible in tokamak plasmas with a realistic q profile. The zonal flow behaviour is changed by the safety factor q. In the low q region where the parallel sound frequency of the (1,0) mode is higher than that of the oscillatory zonal flows, the stationary zonal flows are dominant. The stationary zonal flows suppress the turbulence effectively and become dominant over the turbulence. On the other hand, the zonal flows in the high q region oscillate with the (1,0) pressure perturbations. The oscillatory zonal flows are less effective in suppressing the turbulence. The both types of zonal flows are driven by the Reynolds stress. In the quasi steady state the zonal flow energy supplied by the Reynolds stress goes to the (1,0) pressure perturbations via the geodesic transfer. For the stationary zonal flows the zonal flow energy goes to the (1,0) parallel flows through the (1,0) pressure perturbations. On the other hand, the energy transferred from the oscillatory zonal flows to the (1,0) pressure perturbations is mainly consumed by the nonlinear transfer to the ITG turbulence as well as the Landau damping.

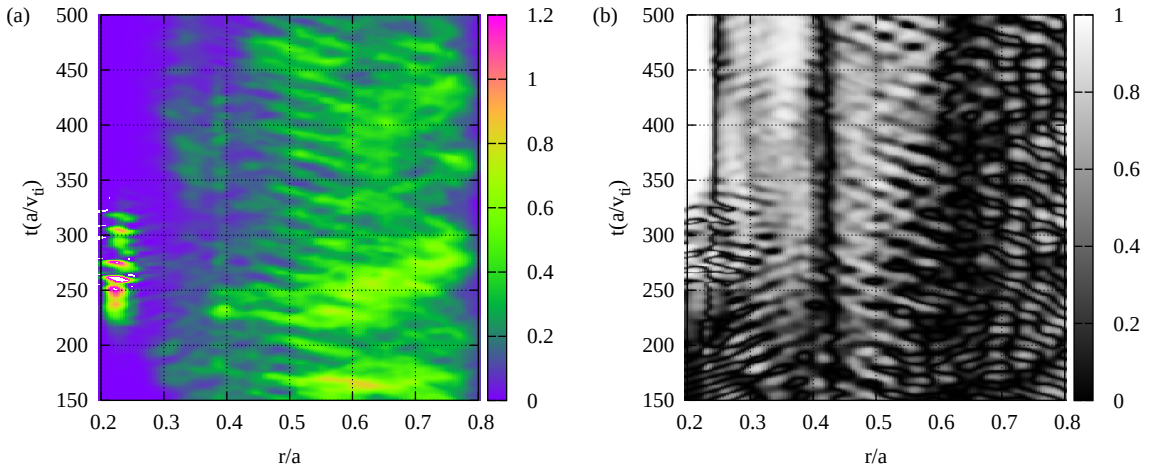

FIG. 9: Electrostatic component of heat flux (a) and ratio of zonal flow energy to total $E\times B$ kinetic energy $(d\phi_0/dr)^2/|\nabla\tilde{\phi}|^2$ (b) as a function of radius and time in the case with $q = 1.05 + 2(r/a)^{3.5}$.

The turbulent transport can be controlled through the control of the zonal flow behaviour by the q profile. These results may be helpful to understand the experimentally observed ITBs, although to investigate a relation with the ITB formation the inclusion of neoclassical effect and heating is necessary like in Refs. [6, 7].

The authors (especially N. M.) would like to thank Dr. M. Yagi, Dr. H. Sugama, Dr. P. B. Snyder, Dr. J. Candy and Dr. G. R. McKee for useful discussions. We also thank Dr. M. Kikuchi and Dr. H. Ninomiya for their support.

References

[1] KISHIMOTO, Y., et al., Proc. 19th IAEA Fusion Energy Conf., Lyon, France, 2002, (IAEA, Vienna, 2002) IAEA-CN-94/TH/1-5.

[2] HALLATSCHEK, K., and BISKAMP, D., Phys. Rev. Lett. **86**, 1223 (2001).

[3] MCKEE, G. R., et al., Phys. Plasmas **10**, 1712 (2003).

[4] SCOTT, B., Phys. Lett. A **320**, 53 (2003).

[5] HAHM, T. S., et al., Phys. Plasmas **6**, 922 (1999).

[6] VOITSEKHOVITCH, I., et al., Phys. Plasmas **9**, 4671 (2002).

[7] THYAGARAJA, A., Plasma Phys. Control. Fusion **42**, B255 (2000).

[8] MIYATO, N., HAMAGUCHI, S. and WAKATANI, M., Plasma Phys. Controlled Fusion **44**, 1689 (2002).

[9] HAMMETT, G. W. and PERKINS, F. W., Phys. Rev. Lett. **64**, 3019 (1990).

[10] SNYDER, P. B. and HAMMETT, G. W., Phys. Plasmas **8**, 3199 (2001).

[11] MIYATO, N., KISHIMOTO, Y. and LI, J., to be published in Phys. Plasmas (2004).

[12] HALLATSCHEK, K., Phys. Rev. Lett. **93**, 065001 (2004).

[13] RAMISCH, M., et al., New J. Phys. **5**, 12.1 (2003).